Astron. Astrophys. 285, 663–674 (1994)

ASTRONOMY AND ASTROPHYSICS

Non-linear properties of the dynamics of bursts and flares in the solar and stellar coronae

H. Isliker and A.O. Benz

Institute of Astronomy, ETH-Zentrum, CH-8092 Zurich, Switzerland

Received 19 July 1993 / Accepted 5 October 1993

Abstract. Solar and stellar flares are highly structured in space and in time, as is indicated for example by their radio signatures: the narrowband spikes, type III, type II and IV, and pulsation events. Structured in time are also the not flare related type I events (noise storms). The nature of this fragmentation is still not clear. Either, it can be due to stochastic boundary or initial conditions of the respective processes, such as inhomogeneities in the coronal plasma. Or else, a deterministic non-linear process is able to cause complicated patterns of these kinds.

We investigate the nature of the fragmentation in time. The properties of processes we enquire are stationarity, periodicity, intermittency, and, with dimension estimating methods, we try to discriminate between stochasticism and low-dimensional determinism. Since the measured time series are rather short, the dimension estimate methods have to be used with care: we have developed an extended dimension estimate procedure consisting of five steps. Among others, it comprises again the questions of stationarity and intermittency, but also the more technical problems of temporal correlations, judging scaling and convergence, and few data points (statistical limits).

We investigate 3 events of narrowband spikes, 13 type III groups, 10 type I storms, 3 type II bursts and 1 type IV event of solar origin, and 3 pulsation-like events of stellar origin. They have in common that all of them have stationary phases, periodicities are rather seldom, and intermittency is quite abundant. However, the burst types turn out to have different characteristics. None of the investigated time series reveals a low-dimensional behaviour. This implies that they originate from complex processes having dimensions (degrees of freedom) greater than about 4 to 6, which includes infinity, i.e. stochasticity. The lower limit of the degrees of freedom is inferred from numerical experiments with known chaotic systems, using time series of similar lengths, and it depends slightly on the burst types.

Key words: Sun: flares – stars: flare – Sun: radio radiation – chaotic phenomena – methods: data analysis – methods: statistical

Send offprint requests to: H. Isliker

1. Introduction

Free magnetic energy is released in the solar corona in the form of several types of flares and in noise storms. Flares on single K and M stars are several orders of magnitudes more powerful; they are generally believed to be caused by the same processes. Some radio emissions of flares and noise storms are produced by coherent mechanisms. The radiations are characterized by generally high polarization and relatively narrow bandwidth. They appear in multiple bursts at different frequencies and are usually much more structured in time than the hard X-ray emission (incoherent bremsstrahlung of single electrons). What causes the fragmentation of the radio emissions? At which stage between the primary energy release, particle acceleration, particle propagation, emission process and radiation propagation does the fragmentation occur?

In this paper we investigate the time evolution of the emissions. We consider general properties of the system dynamics, observed in time series, namely stationarity, intermittency, periodicity and low-dimensional chaos. They are related to interpreting the time variability by opposite scenarios: (i) The source may be controlled by a *stochastic* input. This would be the case, for example, if stochastic fluctuations in the upstream plasma of a shock drive the source, or if the emission process spreads out spatially like a chain-reaction in a stochastically inhomogeneous medium. (ii) On the other hand, the source may be an independent system fully determined by non-linear equations of several variables and behave (iia) periodic or quasi-periodic, or (iib) *deterministic chaotically*. The latter means that it is very sensitive to initial conditions, making it appear irregular. An example of such a system may be the population of magnetically trapped electrons in near equilibrium between loss-cone instability and precipitation. (iii) The source can be in a non-stationary transient state, having not yet settled down to one of the other possible states.

The only burst type which has been enquired with respect to some of the mentioned questions and for which low-dimensional chaotic behaviour is claimed are decimetric pulsations (Kurths & Herzel 1987; Kurths et al. 1991). They are the most regular burst type. Pulsations are not further investigated here.

We use different tools from dynamic systems theory: (i) In the reconstructed phase space of a system, we perform a stationarity test. Only stationary data are suited for any further investigation. (ii) We calculate power spectra to search for the presence of modes. (iii) Intermittency is looked for. It often is obvious, but not easy to quantify in a general way. (iv) In order to discern between stochastic and deterministic processes, correlation dimensions are estimated in phase space. High dimensional deterministic behaviour, however, cannot be distinguished from stochasticity.

Dimension estimate has some intricacies which should not be underestimated, for they can even yield spurious dimensions. Two of them are banned by analyzing only stationary sections and by taking care of possible intermittency. There are three more dangers of a technical kind: (i) The data can be too short or too noisy for a dimension estimate. (ii) Temporal instead of the wanted spatial correlations in phase space may dominate the estimate algorithms. (iii) Scaling and convergence of the involved algorithms can be hard to judge. We have taken into account all these points by developing new tools supplementing the dimension estimate, and by experimenting with numerically produced data.

Coherent radio bursts are classified into different types representing distinct emission processes and source properties (e.g. McLean & Labrum 1985; Güdel & Benz 1988). It is therefore conceivable that the various types (i.e. their sources) exhibit different behaviours. The following burst types are suitable for a dimensional analysis and have been investigated:

1. *Type I bursts* of solar noise storms are believed to be a result of the interaction of newly emerging magnetic flux with the pre-existing coronal magnetic field (Benz & Wentzel 1981).
2. Radio emission of coronal shock waves (*type II bursts*) originates from particles accelerated at the shock front (e.g. Holman & Pesses 1983).
3. Solar flares sometimes produce hundreds of electron beams, each emitting a *type III radio burst* by beam-plasma interactions.
4. *Type IV* events are long lasting broadband continua, evidence of a cloud of hot particles behind a shock front. They can exhibit temporal fine structure, superimposed on a slowly varying background.
5. Extremely narrowband *spikes* of a few hundredths of a second duration appear in groups of thousands during flares. The emission may be at a harmonic of the electron gyrofrequency, but the origin is not known (review by Benz 1986).
6. We also analyze strongly variable radio emission from *stellar flares*. The bursts resemble solar decimetric pulsations.

The data are briefly described in Sect. 2. Section 3 introduces the used tools. Section 3.5. summarizes the whole procedure and the steps of our extended dimension estimate method. The results are presented in Sect. 4, their astrophysical impact is discussed in Sect. 5, the conclusion.

2. The investigated data

The solar radio data have been recorded by the frequency-agile radio spectrometer IKARUS at ETH Zurich, between 1980 and 1982. The instrument is described by Perrenoud (1982). It can be changed in steps from measuring 200 frequencies in the range 100 to 1000 MHz with time resolution 0.1 sec, to measuring 1 frequency channel at 0.5 ms resolution. This allows to measure any burst type at a time resolution adequate for dimensional analysis, i.e. every peak or spike is resolved by 10 to 30 data points.

The data we use are representative for the particular burst types. We were not able to find any data which are substantially longer or better suitable for the present analysis than the ones presented in this article, searching in the data stock of the spectrometers IKARUS and PHOENIX (described in Benz et al. 1991) which covers the period from 1979 to 1993.

The stellar data are flares of the dMe star AD Leo, observed in Arecibo in November 1987 by Bookbinder & Bastian. They are published in Bastian et al. (1990) and Guedel et al. (1989). Time resolution is 20 ms, and the original 256 channels were averaged to a single channel of 40 MHz bandwidth, centered at 1415 MHz, for both left and right circular polarization.

3. Phase space and used methods

The theory of dynamical systems is generally formulated in phase space (state space), whose coordinates are the system variables. The evolution of a process corresponds to a motion in this space. Measuring the radio flux of an event, we observe one coordinate of phase space in the form of data points $X(t_i)$ at the times t_i ($i = 1, ..., N$). By a theorem of Takens (1981) the entire phase space can be reconstructed: From a given time series $\{X(t_i)\}_{i=1}^{N}$, vectors $\boldsymbol{\xi}(t_i)$ are built up in a d-dimensional space as

$$\boldsymbol{\xi}(t_i) := \Big[\, X(t_i),\, X(t_i + \Delta t), ..., X(t_i + (d-1)\Delta t) \,\Big]. \qquad (1)$$

These vectors define the reconstructed phase space. The time delay Δt is a multiple of the time resolution $\tau = t_{i+1} - t_i$. The real phase space of dimension D is embedded in this reconstructed space whenever $d > 2D + 1$.

Takens theorem makes phase space motion accessible. What does this motion look like? On one hand, a limit set of a process' motion may exist, the so-called attractor. It is the set covered by the trajectories after the transient motions have died out and the system has settled down to a *stationary* state. This stationary process can be quasi-periodic with k modes, then it moves on a k-dimensional torus; or it can be stochastic and erratically bounce and fill an entire subset of phase space whose dimension equals the one of the embedding space, d — if the system is bounded and recurrent, which is guaranteed by stationarity. In between lie the chaotic processes. They are deterministic, however non-linear, which, in their case, leads to a sensitive dependence on initial conditions, an exponentially fast separation

of nearby trajectories. This stretching of the trajectories in phase space, combined with the shrinking of the attractor volume in case of a dissipative system, can produce a highly intricate set, very often having a power-law scaling of the data point distribution with a fractal exponent. Therefore, a fractal dimension D of the limit set smaller than the dimension d of the embedding space is indicative of a deterministic non-linear chaotic process. The dimension itself is a measure of complexity of the system. It corresponds to the minimum number of variables needed to describe the system since, for geometrical reasons, the dimension is a lower limit to the degrees of freedom of the motion. An upper limit cannot be inferred.

These three classes of stationary processes can be intermittent, no matter whether they are deterministic or stochastic.

On the other hand, there may be no stationary limit set. Then the system is either in a transient phase, and it has not yet settled down to a new limit set, or it is an inherently non-stationary process, as for instance fractional Brownian motion.

3.1. A stationarity test

Stationarity in the strong sense is the property that all statistical moments are independent of time. In other words, a stationary process does not change in time if only its statistical properties are considered. It is stable in a global sense and bounded in phase space. Runaway or transient processes are not stationary.

How to judge stationarity without testing an infinite number of statistical moments? Power spectrum or variance of a time series are not efficient to investigate stationarity, they contain too little information. We use a *test of stationarity* proposed by Isliker & Kurths (1993) formulating a necessary condition for stationarity. It is based on the invariant measure ρ, operationally defined as the average of Dirac δ-functions along a trajectory $\boldsymbol{x}(t)$ in phase space,

$$\rho := \lim_{T\to\infty} \frac{1}{T} \int_0^T \delta_{\boldsymbol{x}(t)}\, dt, \tag{2}$$

(Eckmann & Ruelle 1985). Equation (2) defines a density measuring how frequently the various parts of phase space are visited by the system. This ρ should clearly be independent of time in a stationary process. To have a better statistics, the projection $\rho(dx_1)$ of $\rho(d\boldsymbol{x})$ onto the flux axis (say x_1) is used:

$$\rho(dx_1) := \int \rho(dx_2 dx_3 ... dx_n). \tag{3}$$

Empirically $\rho(dx_1)$ is calculated by dividing the flux into intervals and counting the flux values falling into these intervals. The measure ρ is a frequency distribution of the flux values.

For a stationarity test one systematically analyzes sections out of a time series. In each section, $\rho(dx_1)$ is calculated for the entire section and for the first half of it. The two distributions are then compared by a χ^2-test. The significance level of the χ^2-test is the confidence with which the density ρ has not changed and is compatible with stationarity. The particular section will be considered stationary in the following. The procedure finally yields a list of parts of a time series which are stationary, as is visualized for a type II event in Fig. 1a. The three largest stationary sections are marked with horizontal dashed or dotted bars. Only stationary data are further analyzed.

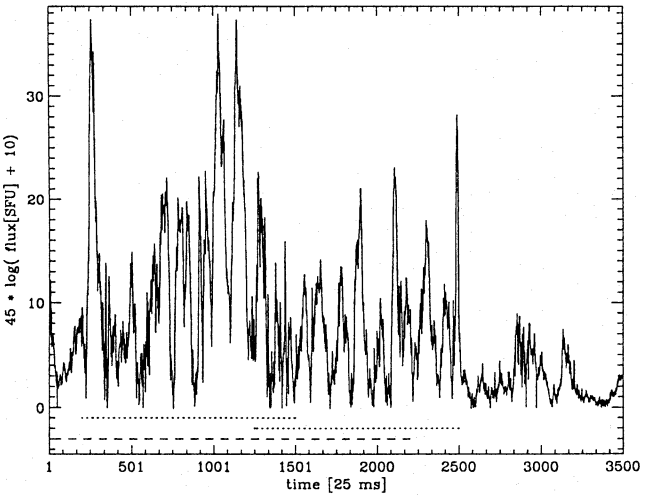

Fig. 1a. The type II event 80/02/28, 12:06:28, observed by a Zurich radio spectrometer with a time resolution of 25 ms. The largest stationary sections are marked with dotted lines, or with a dashed line where a dominating period was found. Eventual stationary subsections of a stationary section are not marked

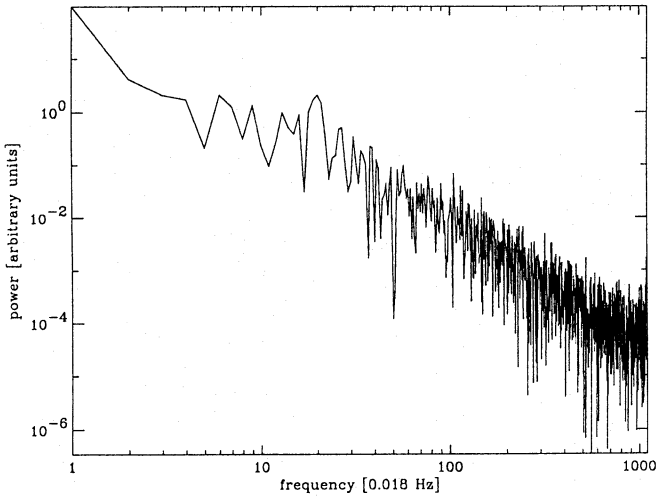

Fig. 1b. Power spectrum of the part of Fig. 1a which is marked by a dashed line

3.2. Power spectrum

We use a standard Fast Fourier Transform (FFT) to calculate the power spectrum. Fig. 1b shows an example of a power spectrum, calculated from a stationary part of the type II event shown in Fig. 1a (the part is marked in this figure with a dashed line). There is a weakly enhanced frequency at 0.34 Hz which can also be recognized in the autocorrelation function.

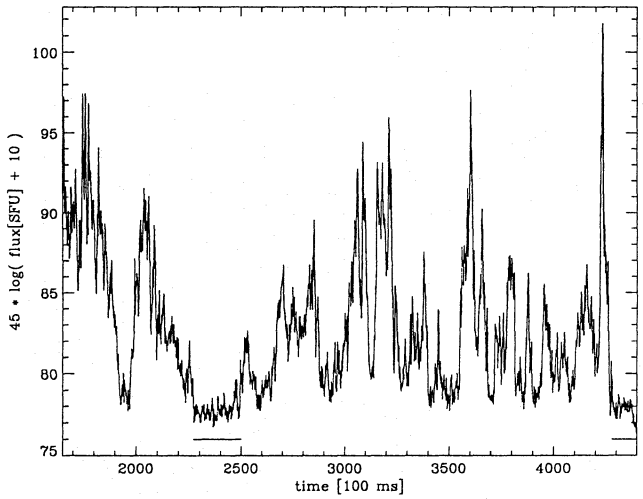

Fig. 2a. The part 1650-4400 of the time series of the type III event 81/11/15, 07:54:44, observed by a Zurich radio spectrometer with a time resolution of 100 ms. The section is stationary, but intermittent. The quiet phases are marked with a bar

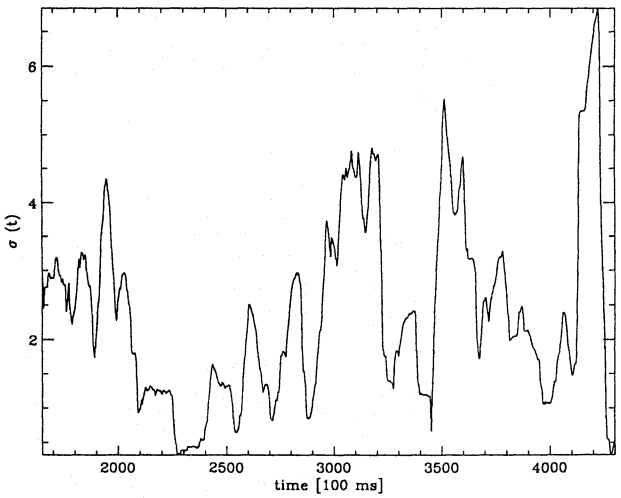

Fig. 2b. For the time series in Fig. 2a, the variance $\sigma(t)$ is shown, in the units of Fig. 2a. The variance was averaged over a window of a length of 100 pixels, corresponding to 5 times the auto-correlation time

3.3. Intermittency

Intermittency is the phenomenon that a time series is interrupted with one or many quiet phases of arbitrary lengths, or with phases of smaller amplitudes (intensities). Figure 2a shows as an example the pixels 1650-4400 of the time series of the type III event 81/11/15, 07:54:44. Two quiet phases are marked with an underlying bar. Intermittent time series can of course be stationary. The stationarity test (Sect. 3.1.) ignores occasional intermittency. In the case of the data in Fig. 2a it has indicated stationarity.

Intermittency is difficult to quantify, as it can appear in many forms. One can find it sometimes by calculating the variances $\sigma(t)$ in a window moving through the time series. An example is given in Fig. 2b. The intermittent phases reveal themselves by reduced variances in a certain time range. An upper limit on $\sigma(t)$, in the units of Fig. 2b about 1.5, may serve to identify quiet intervals. Since $\sigma(t)$ is calculated from a finite window length, the duration of the minima of $\sigma(t)$ are shorter than the quiet intervals. The window's size has to be chosen carefully, a few times the auto-correlation time is most adequate. It turned out that another good way to identify intermittency is by looking simply at the time series.

3.4. Correlation dimensions

3.4.1. Two algorithms to estimate dimensions

We calculate the correlation dimension $D^{(2)}$ which is one out of many definitions of fractal dimension. It is defined as the exponent of a scaling behaviour:

$$P(\epsilon) \sim \epsilon^{D^{(2)}}, \qquad \text{for } \epsilon \to 0, \tag{4}$$

where

$$P(\epsilon) := \text{prob}\ \left[|\boldsymbol{\xi}(t_i) - \boldsymbol{\xi}(t_j)| \leq \epsilon\right] \tag{5}$$

is the distribution of distances. There are two common ways to find $D^{(2)}$:

(α) — In the Grassberger Procaccia method (GP; 1983a, 1983b), the probability term in Eq. (5) is estimated by counting excess distances, $P(\epsilon)$ is replaced by the correlation integral

$$C_d^{(2)}(\epsilon) := \lim_{N\to\infty} \frac{2}{N(N-1)} \sum_{i+W<j}^{N} \Theta\left(\epsilon - |\boldsymbol{\xi}_i - \boldsymbol{\xi}_j|\right), \tag{6}$$

with the Heaviside function $\Theta(.)$ and any vector norm '$|.|$'. Looking for a power-law scaling range, the embedding dimension d has to be successively increased, until convergence, if any, is reached. Several time delays Δt varying around the auto-correlation time t_{corr} have to be tried. The parameter 'W' is discussed in Sect. 3.4.2.C.

(β) — An alternative way to estimate dimensions is the Maximum Likelihood Estimate (ML) (Takens 1984; Ellner 1988). $P(\epsilon)$ in Eqs. (2) and (3) is interpreted as a probability distribution with parameter $D^{(2)}$. This parameter can therefore be calculated by the maximum likelihood method: Assume convergence for $\gamma_1 \leq \epsilon \leq \gamma_2$. Then the usual formalism leads to

$$D^{(2)} = -\frac{n-K}{\sum_{ij=1}^{n} \ln\left(\rho_{ij}/\gamma_2\right)}, \tag{7}$$

where the n distances $\rho_{ij} := \max\left[|\boldsymbol{\xi}(t_i) - \boldsymbol{\xi}(t_j)|\,;\,\gamma_1\right]$ are chosen at random, with the additional constraint that $|t_i - t_j| > W$ (the reason is given in Sect. 3.4.2.C). K is the number of ρ_{ij}'s that are equal to γ_1. Distances $\rho_{ij} > \gamma_2$ are simply omitted. Ellner (1988) shows that if $n = N/2$ the estimate is best, since the distances then are most likely to be independent (N is the length of the original time series).

Mostly, the *error estimate* of correlation dimensions is done in the context of the GP algorithm, using the error of a regression into the relation $\log C_d^{(2)}(\epsilon) - \log \epsilon$. This, however, is not

an intrinsic error. On the other hand, the ML method provides an intrinsic error estimate, in that it fully uses the probabilistic point of view (Ellner 1988) : calculating the mean and standard deviation of the distribution $\epsilon^{D^{(2)}}$ (in Eq. 4), and using the Gaussian law of error propagation, the error in the estimated parameter $D^{(2)}$ of the distribution gets

$$\Delta = \frac{D^{(2)}\ 1.96}{\sqrt{n}} \frac{\sqrt{1+2\ln r_0^{D^{(2)}}\ r_0^{D^{(2)}} - r_0^{2D^{(2)}}}}{1+\ln r_0^{D^{(2)}}\ r_0^{D^{(2)}} - r_0^{D^{(2)}}}, \tag{8}$$

with $r_0 := \gamma_1/\gamma_2$. The factor 1.96 stems from a 5% confidence interval used here.

3.4.2. Dangers of dimension estimate

There are serious sources of misinterpretation of the results of dimension estimates, particularly in astronomy. The critical points which all have an essential influence on dimension estimates are:

- Numerical problems:
  - The data usually are short and unique.
  - The data are noisy. Noise hides the details in the dynamics of the system.
- Non-stationarity;
- Temporal correlations;
- Intermittency: its influence can mimic a finite dimension;
- Problems with interpretation: are the algorithms really converging?

A. Repetitivity: Length of data; noise level. In order to characterize a process globally, a minimum amount of information must be given, i.e. a minimum number of orbits or cycles in phase space, which means a minimum number of peaks in the time series.

It has been claimed from theoretical arguments that the number of points N in a time series should fulfil the relation $N \gtrsim 10^{D^{(2)}/2}$ in order to detect a correlation dimension $D^{(2)}$ (Brandstater & Swinney 1987; Ruelle 1990; Eckmann & Ruelle 1992). Practical inquiries by Isliker (1992a) and newer experiments using the Mackey Glass attractor, however, show that $N \approx 1000$ can deliver reliable, though not very precise results for dimensions smaller than about 4. We found that a lower limit on the number N of points is not crucial. The important quantity is n_S, the number of peaks or structures, defined as

$$n_S := \frac{N\tau}{t_{corr}}, \tag{9}$$

where t_{corr}, the auto-correlation time, is the first minimum of the auto-correlation function, and τ denotes the time resolution. If

$$n_s \gtrsim 50, \tag{10}$$

dimensions up to about 3.5 are reliably estimated, and up to 5 they are detected. A necessary condition is that the number of data points per structure (cycle) is between about 10 and 30:

$$10 \lesssim t_{corr}/\tau \lesssim 30, \tag{11}$$

with τ being the time resolution.

If the data are around the critical minimum of $n_S \approx 50$ and the GP algorithm converges, there is a possibility that this convergence results from the fact that the considered attractor is not covered with enough points. There may be sparse regions in which the true scaling of the correlation integral breaks down due to the lack of data points. We applied in these cases a 'surrogate data' test: the Fourier transform of the original data is transformed back with random Fourier phases. The surrogate data resemble the original data, they have the same power spectrum and the same auto-correlation function. If some out of a set of different realizations of surrogate data behave the same as the original data in a dimension estimate, then the dimension is almost surely an effect of poor scaling. For a discussion of the surrogate data method see Provenzale et al. (1992).

The noise level, i.e. the ratio noise/signal, should be below about 10% for the evaluation of the correlation dimension (numerical experiments, reported in Isliker 1992a).

B. Stationarity. Stationarity is a prerequisite for deterministic chaos. Non-stationary stochastic processes can yield a finite correlation dimension, e.g. if they are self-affine like fractional Brownian motion (see e.g. Osborne & Provenzale 1989). This dimension is not indicative of deterministic behaviour. Therefore, we only analyze data which pass the stationarity test (Sect. 3.1.).

C. Temporal correlations. The influence of temporal correlations has been studied by Theiler (1986, 1991), who shows that every correlated stochastic process *can* have a finite correlation dimension if only a limited amount of data is accessible. This is caused by pairs of points $\boldsymbol{\xi}_i, \boldsymbol{\xi}_j$ on the attractor which are close in phase space only because they are close in time. Dimensions are then just a measure for temporal correlations, and not for correlations in phase space, i.e. for the structure of a possible attractor.

The influence of temporal correlation can effectively be discarded by forbidding pairs of points closer in time than about the auto-correlation time t_{corr} in the dimension estimate. This is done by introducing the parameter 'W' in the GP procedure (Eq. 6) and the ML procedure (Eq. 7), and letting $W \approx t_{corr}$ (Theiler 1986, 1991).

The parameter W can also be used to test whether a too large section has been analyzed. For large W, say $W \gtrsim N/2$, only pairs of data points from both the ends of the particular section are considered. The middle part is omitted. If a dimension which is finite for $W \approx t_{corr}$ disappears with $W \gtrsim N/2$, it is likely that the ends of the section do not lie on the attractor, though the data have passed the stationarity test (which is no contradiction; stationarity is a more general property than deterministic chaos). We try then to find a smaller stationary section, lying inside the previous one.

D. Intermittency. The intermittent time series of Fig. 2a has passed the stationarity test of Sect. 3.1. A dimension estimate is therefore appropriate, and it yields a finite value. Omitting

vectors from the two marked regions makes the dimension disappear, i.e. beyond detection. The same can be reproduced in the following numerical experiments: The dimension of a stochastic time series of red noise is not finite. If a part of this time series, say 5% or 10%, is replaced by noise of an amplitude about 5 or 10 times smaller, one will find a finite correlation dimension.

Obviously, the finite dimensions of intermittent time series can be due to correlations between vectors from the two different amplitude regimes. Whenever the GP algorithm converges for an intermittent time series, we tried the algorithm again, omitting the vectors from the quiet regime. Several cases occurred where this proved to be important. The finite dimensions disappeared, they were spurious.

E. Test of scaling and convergence. For data produced by a low-dimensional chaotic system, the two algorithms to evaluate the correlation dimension should reveal a proper scaling and they should converge. The latter means that the derived correlation dimension becomes independent of the embedding dimensions for high enough embedding dimensions. However, if the length of the time series is small and the noise level is high, the statistics deteriorates, and scaling and convergence tend to be washed out. Such bad scaling and convergence or divergence is difficult to recognize and judge by eye. We therefore use a test to judge the quality of scaling and convergence, proposed by Isliker (1992a).

The test is based on the idea that the evaluation of dimensions means to search for a power-law scaling of the distribution $C_d^{(2)}(\epsilon)$ (Eq. 6), independent of the embedding dimension d. If scaling in the range $\gamma_1 \leq \epsilon \leq \gamma_2$ is assumed, the ML procedure gives a value $D^{(2)}$, and proposes a distribution $\epsilon^{D^{(2)}}$ in that range. A χ^2-test shows whether the empirical distribution $C_d^{(2)}(\epsilon)$ obeys the postulated distribution. This method is a 'plateau-test'. It checks whether the derivative of the logarithm of the correlation integral $C_d^{(2)}(\epsilon)$ with respect to $\log \epsilon$ is constant in a range of $\log \epsilon$.

The test is modified to take into account two theoretical facts: Badii & Politi (1984) and Smith et al. (1986) have shown that for a lacunar set, i.e. a non-uniform set with sparse regions, the expected scaling of $P(\epsilon)$ (Eq. 4) has to be modified to $P(\epsilon) = \epsilon^{D^{(2)}}\, \psi\left(\ln \epsilon / P\right)$ in order to be realistic. ψ is an unknown periodic function of period 1, P the actual, but unknown period. Furthermore Smith (1988) showed that a plateau must be skew, as a result of the finite size of the attractor.

The test will then check the scaling of the correlation integral, consistency of the GP method with the ML method, and convergence (independence of the embedding dimension).

3.5. Summary of the procedure

We have ordered the above set of methods to yield a systematic way of searching for stationarity, intermittency, periodicities, and dimensions. Figure 3 gives a schematic view of the main points as a summary. The steps of our proceeding are:

1. A time series is selected which is long enough, i.e. $n_S \gtrsim 50$, and which is not dominated by noise (noise level below about 10%).

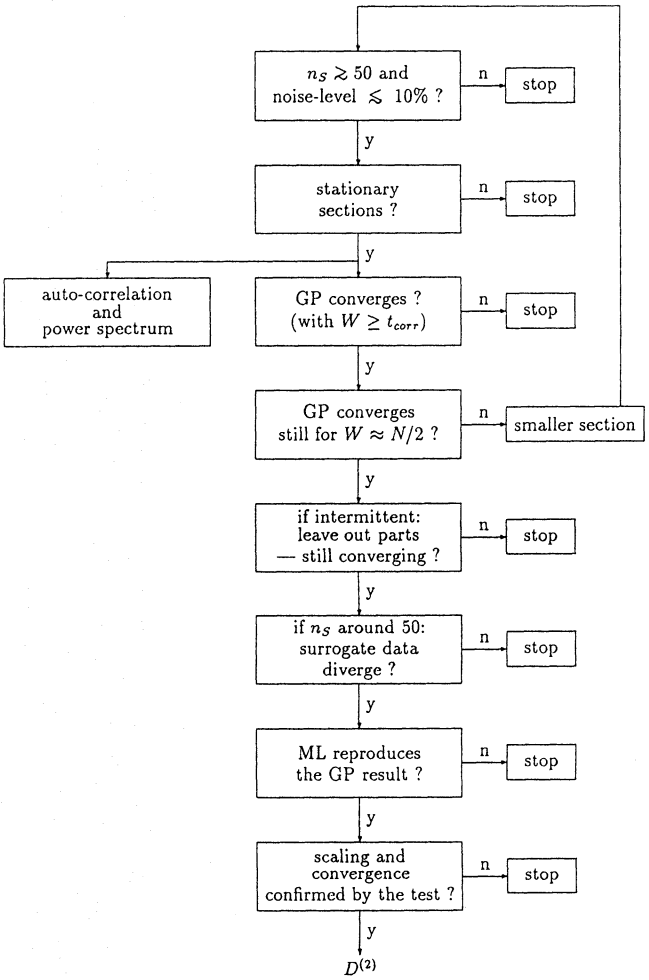

Fig. 3. Schematic view of the main steps of our data analysis, including the extended method used in this paper to estimate correlation dimensions of time series. The scheme is a summary of Sect. 3.5

2. Stationarity of the time series and of subsections of it is checked. All sections must be long enough to satisfy point 1.

The following steps are performed in the stationary sections:

3. The auto-correlation time t_{corr} is estimated.
4. The power-spectrum is calculated to look for the presence of modes.
5. The Grassberger Procaccia algorithm is applied, using $W \gtrsim t_{corr}$, to test for deterministic chaos (Eq. 6). If the GP algorithm converges, we proceed as follows to ensure that the dimension is indicative of deterministic chaos:
   - 5.1. The parameter W is made as large as possible (about $N/2$). If the algorithm diverges now, there may be long ranging time correlations, or the data section is too large. We restart at step 2, with a smaller section. In the other case, if the algorithm still converges, we go on to the next check.
   - 5.2. The data are inspected for possible intermittency. If present, the respective pairs of points are omitted in the evaluation of the correlation integral. If the algorithm

diverges now, the dimension is spurious. If it still converges or if there is no intermittency at all we go on to the next check.

5.3. If the length of the enquired section is around the lower limit, $n_S \approx 50$, the GP algorithm is applied to surrogate data. If there are surrogate data for which the algorithm converges to about the same value as for the original time series, convergence is spurious. Else, we proceed with the following tests.

5.4. Does an ML estimate reproduce the GP result? Only if it does, we go on to the final check.

5.5. The scaling and convergence test is performed. If it confirms the results, the ML estimated value with its error is accepted.

In addition, the dimension analysis is accompanied by:

(a) Two dimensional phase space plots, sometimes three dimensional ones, projected onto a plane, have to be inspected in cases where there is a plateau present: From the $d \log C_d^{(2)}(\epsilon) / d \log \epsilon$ vs. $\log \epsilon$ plot the radii ϵ can be read at which the plateau is situated. In the phase-space plot one can then see whether this radius is characteristic, or whether it is too large and the plateau is a mere edge effect, reflecting saturation of the correlation integral.

(b) In case of dimensions below 3: F^i_{max} vs. F^{i+1}_{max} and d_i vs. d_{i+1} are plotted, where F^i_{max} is the ith local maximum value of the time series and d_i the time between the ith and the $i+1$th maximum. Systems which are that low-dimensional have a good chance to show visible structures.

We furthermore demand consistency of the results with respect to data handling. The effect of standard data modification procedures may be serious or beyond control. Dimensions that appear *only after* an elaborate data modification (such as noise reduction procedures or background subtracting) are not accepted, for such dimensions might just reflect a structure in the modification process, and not in the data.

4. Results and discussion

The results are given in Table 1 with all the necessary details. After date, time, the length of the enquired data, and the frequency, the stationary sections are listed. We also state whether we found any periods in the power spectrum, and how the GP algorithm behaved. If the reason for divergence is intermittency or lack of points (revealed by the surrogate data test) it is indicated in the table. Occasionally, we also investigated series of stationary subsections of an entry in the table and do not list the results separately if they correspond to the ones of the listed section. Finally, in case of convergence, there is a footnote which tells whether the ML algorithm reproduced the GP result, whether the plateau (scaling) and convergence are confirmed by the scaling and convergence test.

General remarks holding for the analysis of all the burst types

(a) Often, neighbouring frequency channels were integrated in order to reduce the noise level. This lowers the frequency resolution. Therefore we integrate just ranges over which the features of a burst do not substantially change.

(b) Often, a data set as a whole appears non-stationary, it looks like elementary bursts (peaks) on a slowly varying background. We refused, however, to subtract an estimated background unless the spectrogram indicates a background to be present, i.e. unless there is increased flux in an interval without bursts. Very likely, the background-like fluctuations stem from the mere superposition of elementary bursts. Exceptions are the type II and the type IV events (see below).

(c) Sometimes, we concatenated data separated by a time gap, pointed out by listing several time ranges in Table 1. This was done in order to get longer time series, however only in cases where the data looked similar, i.e. where the autocorrelation times and the flux amplitudes were comparable.

Results for the different burst types

Type I

Neither periods nor low dimensions were found. Some of the events are intermittent, not always as nicely separable as in Fig. 1. Single bursts can be isolated, separated by short quiet phases. The intermittency test was successful in revealing the true nature of many convergences of the GP algorithm.

Type II

The measurements are time profiles through the main body of a type II burst ('backbone'), which are clearly non-stationary. We therefore subtracted a flexible minimum envelope, to separate the fine structures from the bulk process. This data modification may be justified by the assumption that the bulk and its fine structure have a different physical origin. The type II bursts show no correlation dimensions, the available n_S (Eq. 9) is very short, however. In the 80/2/28 event, we found a moderate peak in the power spectrum, indicating a periodicity of 2.9 seconds (cf. Fig. 1).

Type III

Type III bursts are rather broadband events. A few times it was possible to analyze different frequencies of similar time ranges in the same event. No convergence of the GP algorithm and no periods were found. The stationary sections are relatively short, compared to the other burst types, so we often had to apply the surrogate data test which was often successful in explaining convergence of the GP algorithm. Some type III groups are intermittent.

Type IV

Again a flexible minimum envelope had to be subtracted, yielding stationary and very homogeneous time series. The GP algorithm did not converge, and no periodicities were observed.

Narrowband spikes

No prominent periods and no low-dimensional chaos were found. The first two events in Table 1, 82/6/4 and 82/7/17, are very nicely suited for a dimensional analysis (large data sets, with large stationary sections, low noise level). We found several

Table 1. We list date and start time in UT of the events, time resolution τ, the number of available data points (pixels), and the frequency. Then the stationary sections are given in pixels, as well as the auto-correlation time. Since the latter usually does not vary much during an event, we do not give its value for each stationary section. Eventual periods within stationary sections are reported, and finally the results of the Grassberger-Procaccia algorithm (GP) estimating the correlation dimension. In case of convergence ('conv.'), there is a footnote telling the result of the maximum likelihood estimate (ML) and of the scaling and convergence test (plateau-test). The reason for divergence ('div.') is given if it is intermittency ('interm.') or break-down of scaling ('satur.'), as it is revealed by the surrogate data test

Table 1a. The type I events

Data: Start Time	Resol. τ [ms]	Duration [pixels]	Frequ. [MHz]	Stationary Section from	to	t_{corr} [pixels]	periods T [pixels]	GP
82/ 4/11 : 05:33:57	100	240	247	1	240	8		div.
82/ 4/11: 05:34:54	100	970 (210)	251.5	201	972 [1])	~5		div. (interm.)
05:36:14		(270)						
05:36:45		(490)						
82/ 4/23: 09:08:15	20	3000	262.5	1	750	22		div. (interm.)
				750	2500			div.
				1250	2500			div. (interm.)
				2050	2600			div.
82/ 5/ 7 : 12:28:25	20	12000 (3000)	262.5	1	2500			div. (interm.)
				2000	5000	60		div. (interm.)
12:31:05		(3000)		6500	8500	50		div. (satur.)
12:33:18		(3000)		9000	12000	47		div. (interm.)
12:41:15		(3000)				30		
82/ 9/11 : 10:08:19	20	3000	262.5	500	1400	30		div.
82/ 5/ 5 : 12:08:56	60	4000 (1000)	262.5	250	1500			div.
				500	1750	11		conv. [2])
16:35:46		(1000)		1750	3000	17		div.
16:55:00		(1000)		2000	3000	~ 7		div.
16:58:46		(1000)				13		
82/ 5/ 7: \05:06:20	60	1000	262.5	200	900	7		interm.
82/ 5/ 7 : 08:30:34	60	1000	262.5	1	300	5		div.
				350	1000			interm.
82/ 5/ 6: 09:52:59	60	3000 (1000)	262.5	1	3000	9		div. (interm.)
				200	1300			div. (interm.)
10:42:42		(1000)		2200	2800			div.
10:45:21		(1000)						
82/ 5/ 7 : 12:52:52	80	2250 (750)	262.5	1	1250	11		div.
				250	750			div.
13:08:52		(750)		1000	1500			div. (interm.)
13:11:40		(750)		1250	2250			interm.
				and subsections				interm.

[1]) The quiet part 221 – 270 has been omitted.
[2]) Approximately reproduced by ML, but not confirmed by the scaling and convergence test.

Table 1b. The type II events

Data: Start Time	Resol. τ [ms]	Duration [pixels]	Frequ. [MHz]	Stationary Section from	to	t_{corr} [pixels]	periods T [pixels]	GP
80/ 2/28 : 12:06:28	25	3520	468	1	2200	68	$\approx$ 116 [1])	div.
				200	1500			div.
				1250	2500			div.
82/ 6/ 4 : 06:32:56	20	3000	262.5	600	2900	100		div.
82/ 6/ 4 : 06:33:57	20	3000	362.5	1	1000	46		div.
				350	2500			div.
				subsections				div.

[1]) weak

sections where the GP algorithm converged, it turned out, however, that it was a subtle effect of intermittency. This corrects the enquiry on narrowband spikes by Isliker (1992b), whose results were not gained with the present extended dimension-estimate

Table 1c. The type III events

Data: Start Time	Resol. τ [ms]	Duration [pixels]	Frequ. [MHz]	Stationary Section from	to	t_{corr} [pixels]	periods T [pixels]	GP
82/ 4/18 : 05:45:00	100	1210	119.5	400	1150	20		div. (satur.)
			251.5	250	1200			interm.
			"	500	1000			div. (interm.)
81/ 2/ 3 : 10:44:58	100	950	452.5	1	950	12		div.
				and subsections				div.
82/ 6/ 6 : 12:30:01	20	3000	262.5	1750	2900	65		div.
				and subsections				div.
82/ 9/17 : 07:31:53	20	3000	262.5	1050	2200	45		div. (satur.)
82/ 9/17 : 07:34:02	20	3000	262.5	200	1800	45		div. (satur.)
81/10/07 : 10:33:42	100	2492	317.5	200	1850	33		div.
				500	1700			div. (interm.)
81/11/15 : 07:54:44	100	5760	257.5	800	2250	20		interm.
				1650	4400			interm.
				and subsections				div. (interm.)
81/11/15 : 13:14:50	100	3212	239.5	350	1800	20		div.
			"	many subsections				div.
			377.5	250	1650			div.
			"	900	1900			div.
			"	1350	2000			div. (interm.)
80/06/27 : 16:14:18	100	1750	244	750	1750	18		div.
			"	subsections				div.
			277	1	650			interm.
			"	750	1700			div.
			"	and subsections				div.
			310	1150	1700			div.
82/ 4/ 7 : 12:19:34	100	2080	257.5	200	800	15		div.
12:20:02			"	750	1750			div.
12:21:04			"	and subsections				div.
12:22:06			287.5	1	1350			div.
12:23:20			"	and subsections				div.
12:23:57			"	500	1950			div.
			"	and subsections				div.
			317.5	1000	1300			div.
			"	1150	1500			div.
82/ 4/14 : 06:04:14	100	1232	377.5	20	640	19		div.
06:05:11				420	940			div.
06:06:00				660	1200			div.
06:06:35								
82/ 4/16 : 13:08:10	100	1640	257.5	1	400			div.
13:10:01		(480)	"	500	1300	10		div.
		(1160)	"	1100	1600	25		div.
			287.5	1	400			div.
			"	681	1240			div.
			"	1160	1640			div.
			377.5	600	1220			div.
82/ 4/16 : 14:15:55	100	800	257.5	310	660	12		div.
			287.5	61	680			div.
			317.5	61	680			div.

method. The third event, 82/12/16, has to be treated more cautiously. Though it is very long, the time resolution is lower, and the noise level is higher. This inhibits experimenting with the data (varying the time delay or integrating the data). A possible low dimension might remain hidden due to the non-optimum state of the data.

Stellar flares

The data have a very high noise level, therefore we had to apply a noise reduction in order to be able to search for dimensions at all. We used an iterated Wiener filter, which subtracts noise in Fourier space. Simpler methods, such as boxcar smoothing, were also tried. Such methods are known to be able to reduce the complexity of a process, more concrete, dimensions can be lowered, if present. It is not clear, whether they can even remove dimensions completely. Most stationary sections show a slight peak in the power spectrum. Usually, one expects periods to be reflected in a dimensional analysis as a dimension 1 (or 2 if two independent frequencies are present). This was not the case here, the dimensions seem to be hidden in the noise.

Table 1d. The type IV event

Data: Start Time	Resol. τ [ms]	Duration [pixels]	Frequ. [MHz]	Stationary Section from	to	t_{corr} [pixels]	periods T [pixels]	GP
80/ 4/ 6 : 14:24:30	300	1103	444.5	83	1100	27		div.
			616	1	833			div.

Table 1e. The narrowband-spike events

Data: Start Time	Resol. τ [ms]	Duration [pixels]	Frequ. [Mhz]	Stationary Section from	to	t_{corr} [pixels]	periods T [pixels]	GP
82/ 6/ 4 : 13:38:41	4	8250	363	1500	8250	33		
				many subsections				div. (some interm.)
				1500	4000			div.
				4000	8250			div.
82/ 7/17 : 10:06:26	2	10000	770	1	1000	20		div.
				1000	4000			div.
				5000	6000			div.
				6000	10500 [1]			div.
82/12/16 : 10:04:22	10	12000	730	1	12000	9		div.
				many subsections				div.
	10		870	1	12000	4		div.
				many subsections				div.
	10		1010	1000	11000	3		div.
				many subsections				div.

[1]) The quiet sections 7000-7200 and 7700-7800 have been omitted.

Statistics of the results

A more condensed summary of the results is given by Table 2. The first entry is the ratio $t(stat.)/t(all)$, where $t(all)$ is the total amount of time covered by the measurements, and $t(stat.)$ is the total amount of time where the systems were in a stationary state. This ratio is not necessarily a characteristic of the particular burst types: it mainly reflects the effectiveness of the data selection from our data base. The data were categorized into 'apt for analysis' and 'not apt for analysis', without any mathematical method.

The next entry, however, $\bar{n}_S(stat.)$, the average length of stationary sections in units of the respective auto-correlation time, is a characteristic of the different burst types. The narrowband spikes, type I and stellar flares have the longest stationary sections, where the large value for the narrowband spikes is due to the 82/12/16 event. Without this exceptional case, $\bar{n}_S(stat.)$ equals 133 ± 79. Only the statistics for type I and type III is relatively good, as is seen from inspection of Table 1.

Since the GP algorithm was not observed to converge, we can infer that there is no low-dimensional chaos. The processes are high dimensional, with the dimensions so high that the length of the time series does not allow to detect them. The numerical experiments of Isliker (1992a, see Sect. 3.4.2) and similar unpublished experiments with known chaotic systems give a very rough estimate of the lower limit for the respective dimensions. This value $D^{(2)}_{min}$ is given in Table 2. It should be interpreted in the sense that the correlation dimension of for instance a type I event must be expected to be larger than 5. Of course, this includes infinity, i.e. stochasticity. The type II's and type IV's limits are in brackets, since the statistics is too poor for a definite answer. The noise in the stellar data prohibits to give a lower limit.

5. Conclusion

All burst types have been found in stationary states for some time. How long these states last depends on the individual burst types. The type I events, narrowband spikes and stellar flares have the longest stationary states. It is therefore adequate to search for physical models which are able to bring forth stationary solutions, as e.g. electron cyclotron masers, or quasi-steady reconnection, two models which are in discussion for the latter two burst types.

The stationary sections of type II, type III and type IV bursts are so short that the transient states at the beginning and at the end have to be taken into account. This means that the start phase and the decay phase of the operating processes are a relevant part of any available measurement, and they hardly can be neglected in the models.

The narrowband spikes and type I events have a tendency to be interrupted in their long stationary phases. These short intermittencies are short lasting suppressions of the emission mechanism. Type III's are less homogeneous, i.e. intermittency is present not just in the form of stopped emission, but also in the form of reduced amplitudes. Type II and type IV events are mixed, some are homogeneous, some are not. The stellar flares are not intermittent. Concerning models, we note that there are examples of non-linear stochastic processes (Provenzale et al. 1992), as well as of deterministic equations which show features of intermittency.

Periodicities are rare, except in the pulsation-like stellar flares. They are constantly pulsating, resembling very much solar pulsations. The periods are not very prominent, their power typically is a factor 3 to 10 stronger than the power of the neigh-

Table 1f. The stellar flares (all AD Leo)

Data: Start Time	Resol. τ [ms]	Duration [pixels]	Frequ. [MHz]	Stationary Section from	to	t_{corr} [pixels]	periods T [pixels]	GP
87/11/ 4: 11:04:56.68	20	2184	1415	800	2150	13		div.
				many subsections				div.
87/11/ 4 : 11:13:01.00	20	15124	1415	1	3250	...	≈ 33 [1])	interm.
		(6984)		2250	3000	16		div.
11:15:40.68		(3500)		3750	4500	12	≈ 33 [1])	div.
11:17:00.38		(4640)		6235	6984	18	≈ 33 [1])	div.
				7985	9234		≈ 25 [1])	div.
				8735	9734		≈ 25 [1])	div.
				9985	10734		≈ 25 [1])	div.
				10985	11884		≈ 28 [1])	div.
				12735	13984		≈ 25 [1])	div.
				13635	14884		≈ 28 [1])	div.
87/11/ 7 : 10:55:10.90	20	2000	1415	450	1600	14	≈ 58 and 25 [2])	div.
				1	800		≈ 62 [1])	div.
				300	1100		≈ 53 and 27 [2])	div.
				800	1600		≈ 33 [1])	div.
				1601	2000		≈ 44 and 25 [2])	div.

[1]) weak period , broad peak
[2]) weak period

Table 2. Statistics of the results: In some ms-spikes, type III and pulsation events we have analyzed different frequencies at equal times. Therefore, they have two entries in the table. The entries marked by an asterisk are just the lowest of the accessible frequencies taken into account, whereas the unmarked entry is summing up the different frequencies as if they were different events. The entries are: $\frac{t(stat.)}{t(all)}$, the ratio of stationary phases of the measurements, summed over all events, divided by the total observing time; $\bar{n}_S \equiv < \frac{t(stat.)}{t_{corr}} >$, the average length of a stationary sections in units of the auto-correlation time, $D^{(2)}_{min}$, a rough estimate of the lower limit for the dimensions of the respective processes

	$\frac{t(stat.)}{t(all)}$	$\bar{n}_S \equiv < \frac{t(stat.)}{t_{corr}} >$	$D^{(2)}_{min}$
type I	92.4%	94 $\pm$ 71	5
type II	93.9%	28 $\pm$ 12	(4)
type III *)	69.8%	47 $\pm$ 29	3 - 4
type III	81.7%	46 $\pm$ 26	3 - 4
type IV *)	92.3%	38 $\pm$ 0	(4)
type IV	83.9%	35 $\pm$ 5	(4)
ms-spikes *)	93.3%	333 $\pm$ 495	5
ms-spikes	93.3%	1041 $\pm$ 1380	5
stellar	76.9%	76 $\pm$ 42	?

bouring frequencies. Because of this and because the power spectrum is not at all uniform, these modes do not explain the entire dynamics of a process. It remains unclear whether there is a hidden chaotic or a stochastic process with a dominant mode.

The enquired data are all high-dimensional; low-dimensional chaos has not been detected, therefore

(a) either the dimension is infinite and the system is stochastic (a sum of many uncorrelated processes, or a process governed by stochastic boundary or initial conditions),
(b) or the dimension is finite and the system is high-dimensional deterministic chaotic ($D^{(2)} \gtrsim 4 - 5$).

This latter distinction could be done with dimension estimate methods only if the processes revealed themselves in time series which were substantially longer than the ones considered in this article. It seems, however, that it is the very nature of the respective processes to be restricted to the typical durations reported. The boundary between detectable low dimensions and undetectable high dimensions has to be estimated from numerical experiments on known chaotic systems: the dimensions must be greater than 5 for narrowband spikes and type I events, and greater than 3 or 4 for type III, type II and type IV events. The lower limit remains open for the stellar flares, due to their noisiness.

We first draw conclusions on the radio bursts occurring in the impulsive phase of flares, the type III and the narrowband spike events. They are directly connected to the primary energy release. Groups of type III bursts and narrowband spikes last similar times, typically one minute. Single type III bursts have a much longer duration than the narrowband spike bursts. It is quite natural then that the type III groups appear more transient, whereas the short narrowband-spikes have long phases of stationary bursting. The narrowband spikes would have a better chance to reveal a possible low dimension. They do not, so the relevant process must be complex, i.e. with a dimension higher than about 5. This calls for high-dimensional deterministic or stochastic models.

Later in the flare and probably further away from the acceleration site occur the type II and IV events. Type II bursts are emitted in association with a shock wave emerging from the flare. The fine structures at a fixed frequency (suggesting an approximately constant height in the corona) has in one case a simple structure, namely a weak period. Such an oscillation may be produced by a wave structure in the upstream medium modulating the emission at the shock front.

The type I events are not flare related. They appear in the present analysis similar to the narrowband spikes, with long stationary sections. The analysis infers that the type I storms are complex, with dimensions greater than about 5. They have a stronger tendency to be intermittent than the narrowband spikes. The results exclude a self-contained source model that operates as a non-linear system of a few free variables. The results, on

the contrary, support a scenario for type I storms in which the variability is caused by a stochastic input or a high-dimensional mechanism. Possibilities include inhomogeneous plasma flowing into a reconnection region or activity at a shock front modulated by the upstream medium.

The stellar flares, finally, appear pulsation-like, with long stationary phases and quite strong ordering, as is indicated by the frequent presence of quasi-periodicity. We cannot consider the absence of low-dimensions to be a final result, since the quality of the data is not adequate. Better data is needed, with a lower noise level, or an efficient, but conservative noise reduction method in phase space.

We note that this analysis does not disprove deterministic chaos in the flare radio emission. It merely shows that if deterministic chaos is present in the analyzed data, then it is not low-dimensional. The results of this work give constraints to models for all types of investigated bursts. Stationarity, intermittency and dimensionality are new characteristics of radio bursts which should be taken into account in their interpretation.

Acknowledgements. We thank W. Stehling for his work on the spectrometers IKARUS and PHOENIX, and we thank M. Davis, T.S. Bastian and J. Bookbinder for passing the stellar data to us, and for various help in handling them. This work was supported by the Swiss National Science Foundation (grant No. 2000-5.499).

References

Badii R., Politi A., 1984, Phys. Lett. A 104, 303
Bastian T.S., Bookbinder J., Dulk G.A., Davis M., 1990, ApJ 353, 265
Benz A.O., 1986, Solar Phys. 104, 99
Benz A.O., Güdel M., Isliker H., et al., 1991, Solar Phys. 133, 385
Benz A.O., Wentzel D., 1981, A&A 94, 100
Brandstater A., Swinney H.L., 1987, Phys. Rev. A 35, 2207
Eckmann J.-P., Ruelle D., 1985, Review of Modern Physics 57, 617
Eckmann J.-P., Ruelle D., 1992, Physica D 56, 185
Ellner S., 1988, Phys. Lett. A 133, 128
Grassberger P., Procaccia I., 1983a, Physica 9D, 189
Grassberger P., Procaccia I., 1983b, Phys. Rev. Lett. 50, 346
Güdel M., Benz A.O., 1988, A&AS 75, 243
Güdel M., Benz A.O., Bastian T.S., et al., 1989, A&A 220, L5
Holman G.D., Pesses M.E., 1983, ApJ 267, 837
Isliker H., 1992a, Phys. Lett. A 169, 313
Isliker H., 1992b, Solar Phys. 141, 325
Isliker H., Kurths J., 1993, Intern. J. of Bifurc. and Chaos, in press
Kurths J., Benz A.O., Aschwanden M.J., 1991, A&A 248, 270
Kurths J., Herzel H., 1987, Physica D 25, 165
McLean D.J., Labrum N.R. (eds), 1985, Solar Radiophysics. Cambridge University Press, Cambridge
Osborne A.R., Provenzale A., 1989, Physica D 35, 357
Perrenoud M.R., 1982, Solar Phys. 81, 197
Provenzale A., Smith L.A., Vio R., Murante G., 1992, Physica D 58, 31
Ruelle D., 1990, Proc. R. Soc. Lond. A 427, 241
Smith L.A., 1988, Phys. Lett. A 133, 283
Smith L.A., Fournier J.-D., Spiegel E.A., 1986, Phys. Lett. A 114, 465
Takens F., 1981, in: Dynamical Systems and Turbulence (Lect. Notes Math., vol. 898) Springer, Berlin, p. 366
Takens F., 1984, in: Dynamical systems and turbulence (Lect. Notes Math., vol. 1125) Springer, Berlin, p. 99
Theiler J., 1986, Phys. Rev. A 34, 2427
Theiler J., 1991, Phys. Lett. A 155, 480